

Synthesis and Micellization of Amphiphilic Brush–Coil Block Copolymer Based on Poly(ϵ -caprolactone) and PEGylated Polyphosphoester

Jin-Zhi Du,^{†,‡} Dong-Ping Chen,^{†,‡} Yu-Cai Wang,^{†,‡} Chun-Sheng Xiao,[‡] Yi-Jie Lu,[§]
Jun Wang,^{*,†,‡,||} and Guang-Zhao Zhang^{†,§}

Hefei National Laboratory for Physical Sciences at Microscale, Department of Polymer Science and Engineering, School of Life Sciences, and Department of Chemical Physics, University of Science and Technology of China, Hefei, Anhui 230026, P.R. China

Received December 28, 2005; Revised Manuscript Received April 6, 2006

A novel biodegradable amphiphilic brush–coil block copolymer consisting of poly(ϵ -caprolactone) and PEGylated polyphosphoester was synthesized by ring opening polymerization. The composition and structure of the copolymer were characterized by ¹H NMR, ¹³C NMR, and FT-IR, and the molecular weight and molecular weight distribution were analyzed by gel permeation chromatograph (GPC) measurements to confirm the diblock structure. These amphiphilic copolymers formed micellar structures in water, and the critical micelle concentrations (CMCs) were around 10^{−3} mg/mL, which was determined using pyrene as a fluorescence probe. Transmission electron microscopy (TEM) images showed that the micelles took an approximately spherical shape with core–shell structure, which was further demonstrated by laser light scattering (LLS) technique. The degradation behavior of the polymeric micelle was also investigated in the presence of *Pseudomonas* lipase and characterized by GPC measurement. Such polymer micelles from brush–coil block copolymers are expected to have wide utility in the field of drug delivery.

Introduction

Polymeric micelles formed in an aqueous solution are nanosized supermolecular assemblies of amphiphilic copolymers that are composed of a compact hydrophobic inner core surrounded by a hydrophilic outer shell. Due to their unique structures, polymeric micelles have been investigated in biomedical fields for pharmaceutical or diagnostic applications.^{1–3} Over the past decade, both amphiphilic linear di- or tri-block copolymers and graft copolymers^{4–7} have been utilized to form micellar architectures. Typical examples of these polymeric micellar systems contained hydrophobic components such as biodegradable poly(ϵ -caprolactone),^{1,8} polylactide^{2,9,10} blocks, or nonbiodegradable blocks such as polystyrene.¹¹ In many examples, poly(ethylene glycol) blocks were used as the hydrophilic components though many other polymers such as poly(*N*-isopropylacrylamide)^{12,13} and other polyelectrolytes such as poly(aspartic acid)^{14,15} were also used for stimuli sensitivity concerns.

It has been demonstrated that end-functionalized amphiphilic diblock copolymers, for example, α -acetal-poly(ethylene glycol)-poly(D,L-lactide), which forms a micellar structure and allows the conjugation of pilot molecules at the tethered end of the hydrophilic segment, exhibited promising potential in biomedical applications.^{16,17} Elicited by such linear amphiphilic diblock copolymers, the brush–coil copolymer may possess the advantage of allowing for more functional groups at the end of the

brushes, which could be further modified either chemically or biologically to obtain desired properties. Recently, Schmidt's group reported that brush-coil type amphiphilic block copolymers formed micelles, which were based on poly(methacrylic acid) and polystyrene, synthesized by either metallocene catalysis or atom-transfer radical polymerization (ATRP).^{18–20} This type of micelle composed of nonbiodegradable elements may be limited in biomedical applications. None of micellar structure from the brush–coil block polymer based on degradable polyester has been reported to our best knowledge.

In the present work, we synthesized biodegradable brush–coil amphiphilic block copolymers of PCL and PEGylated PPE. Hydrophilic brushes of nonfunctional monomethoxy poly(ethylene glycol) (mPEG) was selected as a model in this study. Poly(ϵ -caprolactone) (PCL) was chosen as the hydrophobic segment, i.e., coil segment, since it has been used widely in biomedical fields, especially for drug delivery due to its biodegradability, biocompatibility, and high permeability to drugs at body temperature.^{21–23} Polyphosphoester (PPE) was used as the backbone of the hydrophilic block because of its potential in biomedical applications such as in drug and gene delivery and tissue engineering.^{24–27} More importantly in this study, the pentavalent nature of the phosphorus provides a unique channel to introduce hydrophilic PEG brushes.

We adopted a method for PCL and PPE block polymer synthesis reported recently by us²⁸ to develop this kind of brush–coil diblock copolymer as shown in Scheme 1. The structures of copolymers were well characterized by various methods. We also investigated the micellization of such amphiphilic copolymers using LLS, TEM, and a fluorescence probe technique. In addition, the degradation of the polymeric micelle was studied under the catalysis of *Pseudomonas* lipase.

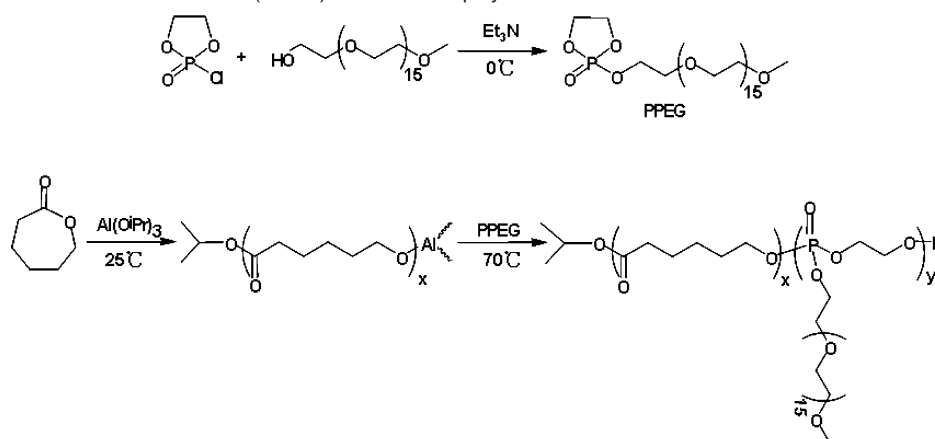
* To whom correspondence should be addressed. E-mail: jwang699@ustc.edu.cn.

[†] Hefei National Laboratory for Physical Sciences at Microscale.

[‡] Department of Polymer Science and Engineering.

[§] Department of Chemical Physics.

^{||} School of Life Sciences.

Scheme 1. Synthesis Procedure of Monomer (PPEG) and Block Copolymer PCL-*b*-PPEG

Experimental Section

2.1. Materials. 2-Chloro-2-oxo-1,3,2-dioxaphospholane (COP) was synthesized by a method described previously²⁹ and distilled under reduced pressure before use. Monomethoxy poly(ethylene glycol) ($M_n = 750$) (mPEG750, Acros Organics, Belgium) was dried twice by azeodistillation of anhydrous benzene. ϵ -Caprolactone (ϵ -CL) (Acros Organics, 99%) was dried over calcium hydride for 48 h at room temperature, followed by distillation under reduced pressure just before use. Aluminum isopropoxide ($\text{Al}(\text{O}^i\text{Pr})_3$) was purified as described in the literature.³⁰ Triethylamine was refluxed with phthalic anhydride, then with potassium hydroxide, and distilled. *Pseudomonas* lipase is a product of Sigma and used without further purification. Benzene, diethyl ether, and toluene were refluxed over phosphorus pentoxide, calcium hydride and sodium, respectively. Pyrene (Acros Organics) and other solvents were used as received.

2.2. Synthesis of PEGylated Phosphoester Monomer (PPEG). To a solution of mPEG750 (21.10 g, 28.13 mmol) and 1 equiv of triethylamine (2.85 g, 28.13 mmol) in 150 mL of anhydrous benzene at 0 °C was added dropwise COP (4.01 g, 28.13 mmol) in 50 mL of anhydrous benzene under magnetic stirring over a period of 1 h. The mixture was maintained at 0 °C for an additional 24 h. The precipitate which was triethylammonium chloride was then filtered off using a Schlenk funnel. The filtrate was concentrated under vacuum and precipitated into 600 mL of cooled anhydrous diethyl ether. The precipitate was collected over the Schlenk funnel and dried under vacuum at room temperature (yield: 70%). ^1H NMR, ^{13}C NMR, ^{31}P NMR spectra, and a single elution peak from GPC analysis supported the structure as shown in the Scheme 1. ^1H NMR (Figure 1A) δ (CDCl_3 ,

ppm): 4.29 (2H, $-\text{POCH}_2\text{CH}_2\text{O}-\text{CH}_2\text{CH}_2\text{O}-$), 4.39 (4H, $-\text{OCH}_2\text{CH}_2\text{O}-$), 3.66 (62H, $-\text{OCH}_2\text{CH}_2\text{O}(\text{CH}_2\text{CH}_2\text{O})_{15}-$), 3.38 (3H, $-\text{OCH}_3$); ^{13}C NMR δ (CDCl_3 , ppm): 58.88 ($-\text{OCH}_3$), 65.96 ($-\text{POCH}_2\text{CH}_2\text{O}-$), 71.82 ($-\text{OCH}_2\text{CH}_2\text{O}-$), 70.46 ($-\text{O}(\text{CH}_2\text{CH}_2\text{O})_{15}-$); ^{31}P NMR (CDCl_3), $\delta = 19.20$ ppm.

2.3. Synthesis of Block Copolymer PCL-*b*-PEGylated PPE (PCL-*b*-PPEG). The brush-coil diblock copolymer was synthesized by consecutive ring-opening polymerization of ϵ -CL and PEGylated phosphoester monomer PPEG using a trimer of $\text{Al}(\text{O}^i\text{Pr})_3$ as an initiator. Briefly, ϵ -CL (2.00 g, 17.5 mmol) and 17.0 mL of dried toluene were introduced into a freshly flamed and nitrogen-purged round-bottom flask through a rubber septum with a stainless steel capillary. To this solution was added the trimer of $\text{Al}(\text{O}^i\text{Pr})_3$ solution at 0.425 mmol/mL (206 μL , 87.6 μmol) in toluene, and the reaction was carried out at 25 °C for 2 h. Then the reactant was equally distributed into two flamed and nitrogen-purged flasks for the polymerization of phosphoester monomer PPEG. After adding PPEG, the reaction was performed at 70 °C for 5 days. The resultant solution was deactivated with 1 mol/L acetic acid and precipitated into an excess of a methanol and diethyl ether mixture (2:1, v/v). The precipitate was dried under vacuum until a constant weight at room temperature to obtain the product. An aliquot before adding PPEG monomer was also taken out, deactivated, and precipitated in cooled methanol for analysis.

2.4. Characterization of PCL-*b*-PPEG Copolymers. ^1H , ^{31}P , and ^{13}C NMR spectra were recorded on a Bruker AV300 NMR spectrometer at room temperature with CDCl_3 as solvent and TMS as internal reference. Phosphoric acid (85%) was used as external reference for ^{31}P NMR analyses. FT-IR spectra were measured on a Bruker Vector 22 Fourier transform infrared spectrometer using the KBr disk method. Molecular weights and molecular weight distributions were determined by gel permeation chromatography (GPC) measurements. The GPC system was composed of a Waters 1515 pump and a Waters 2414 refractive index detector, equipped with Waters Styragel high-resolution columns (HR4, HR2, HR1 \times 2, HR0.5) at 40 °C. THF was used as eluent at the flow rate of 1 mL/min. Monodispersed polystyrene standards were used to generate the calibration curve.

2.5. Preparation of Micelles. Micelles were prepared by the solvent evaporation method. Briefly, 20 mg of copolymer was dissolved in 2 mL of tetrahydrofuran (THF). Under moderate stirring, the predetermined volume of ultra purified water (Millipore, 18.2 M Ω) was added dropwise through a drop funnel, and the mixture was left stirring for an additional 12 h. THF was then removed under reduced pressure at ambient temperature. The final volume of the aqueous solution was adjusted to 10 mL using ultra purified water to obtain polymer micelles.

2.6. Determination of Critical Micelle Concentration (CMC). Critical micelle concentrations of the copolymers were estimated by a fluorescence spectroscopic method using pyrene as the fluorescence probe. A predetermined amount of pyrene solution in acetone was added into a series of volumetric flasks, and the acetone was then evaporated completely. A series of copolymer solutions at different concentrations

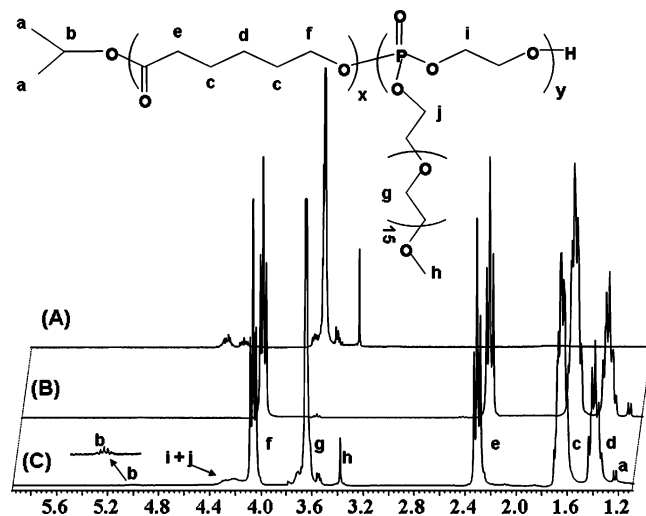


Figure 1. ^1H NMR spectrum (in CDCl_3 , ppm) of (A) PPEG, (B) PCL homopolymer, and (C) PCL-*b*-PPEG copolymer.

ranging from 1.0×10^{-5} to 1.0 mg/mL were added to the bottles, whereas the concentration of pyrene in each flask was fixed at a constant value (6.0×10^{-7} mol/L). The excitation spectra were recorded at 20 °C on a Shimadzu RF-5301PC spectrofluorophotometer with the detection wavelength λ_{em} at 390 nm and a slit width of 3 nm.

2.7. Transmission Electron Microscope (TEM). The morphology examination of the copolymer micelles was performed on a Hitachi model H-800 transmission electron microscope with an accelerating voltage of 200 KV. The sample was prepared by placing a drop of the micelle solution (0.2 mg/mL) onto 230 mesh copper grids coated with carbon and allowing the sample to dry in air before measurement.

2.8. Laser Light Scattering (LLS). Dynamic laser light scattering (DLS) was conducted on a commercial spectrometer (ALV/DLS/SLS-5022F) equipped with an ALV5000 multi- τ digital time correlator and a cylindrical 22 mW UNIPHASE He-Ne laser ($\lambda_0 = 632$ nm) as the light source to characterize the polymeric micelles (0.2 mg/mL) at a scattering angle of 15° and at a constant temperature of 25 °C. Static light scattering (SLS) studies were conducted at 25 °C using the same instrument at scattering angles ranging from 0° to 150°. The micelle solution was filtered using a 0.45 μ m membrane filter prior to measurement for all of the experiments.

2.9. Enzyme Catalyzed Degradation of Polymeric Micelles. The micelles prepared in phosphate buffer (0.05 M, pH 7.0) with a similar procedure as described above at 2.0 mg/mL were incubated with *Pseudomonas* lipase (0.2 mg/mL) at 37 °C. At a predetermined time interval, the sample was taken out and lyophilized. The degradation products were extracted with chloroform and further analyzed by GPC measurements at 40 °C using a set of Waters Styragel high-resolution columns (HR4, HR2, HR1, and HR0.5) and chloroform as the mobile phase.

Results and Discussion

The block copolymer was synthesized according to the procedure shown in Scheme 1. The ring opening polymerization of ϵ -caprolactone using the trimer of aluminum isopropoxide (A_3) as initiator has been studied extensively,^{31,32} which exhibits a well-known living polymerization in toluene. Recently, our laboratory has reported that following ϵ -CL polymerization with trimer of $Al(O^iPr)_3$ in toluene, phosphoester chain can be propagated under the initiation of living PCL macroinitiator and eventually generate the second block polyphosphoester.²⁸ In the present work, we selected mPEG with $M_n = 750$ to react with 2-chloro-2-oxo-1,3,2-dioxaphospholane in the presence of TEA as an acid scavenger. The obtained PEGylated cyclic phosphoester monomer PPEG was well-characterized by 1H (Figure 1A), ^{13}C , and ^{31}P NMR as described in the Experimental Section. We further adopted a similar route as we reported to synthesize the brush-coil PCL and PPEG block copolymer using A_3 as initiator in toluene. During the synthesis, ϵ -caprolactone was first initiated, followed by adding PPEG to the living PCL macroinitiator solution.

Figure 1 shows a comparison of 1H NMR spectra of PPEG, a typical diblock copolymer PCL-*b*-PPEG, and PCL homopolymer. It was found that all signals assigned to protons of PCL block (except for the terminal methylene directly linked to the hydroxyl group) in Figure 1B were also present in the spectrum of block copolymer PCL-*b*-PPEG. Among those newly appearing signals in Figure 1C, resonances at 3.38 (h) and 3.65 ppm (g) can be assigned to protons of the methoxyl group ($-OCH_3$) and methylene protons ($-OCH_2CH_2-$) of the pendant PEG brushes, respectively. In addition, resonances at 4.20–4.30 ppm (i and j) are the characteristic signals of methylene protons ($-POCH_2CH_2O-$) of the phosphoester backbone and the joint methylene protons ($-P-OCH_2CH_2(OCH_2CH_2)_{15}-$) of the PEG brushes.

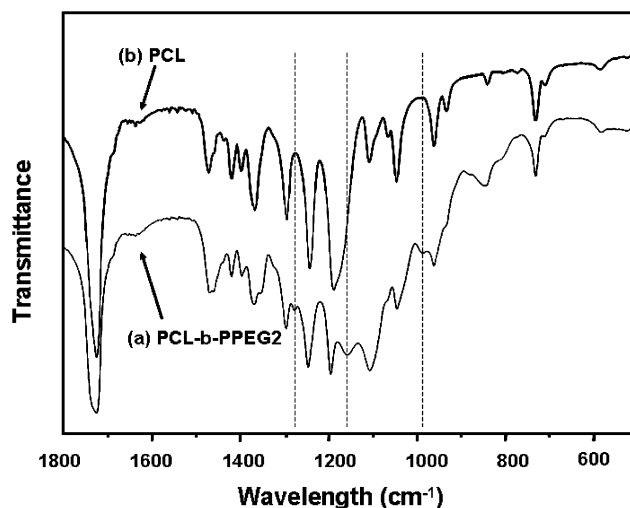


Figure 2. FT-IR spectra of (a) PCL-*b*-PPEG copolymer and (b) PCL homopolymer.

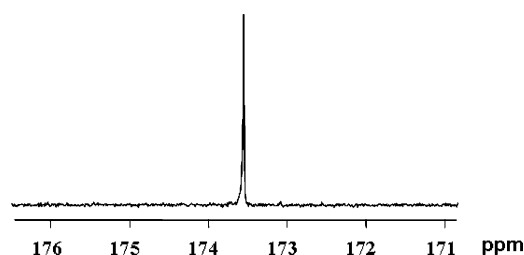


Figure 3. ^{13}C NMR spectrum of carbonyl region of PCL-*b*-PPEG copolymer.

FT-IR analysis results of PCL homopolymer and PCL-*b*-PPEG block polymer were shown in Figure 2. Absorption (bands) at 1276 and 1158 cm^{-1} marked in Figure 2b were observed, which were owed to the asymmetrical and symmetrical P=O stretchings, respectively. The P–O–C stretching was also verified at 988 cm^{-1} in PCL-*b*-PPEG spectrum. Those absorptions, however, were absent in the spectrum of PCL homopolymer. Thus, judging together with analysis by 1H NMR spectrum, it demonstrated the successful polymerization of phosphoester monomers initiated by the PCL macroinitiator.

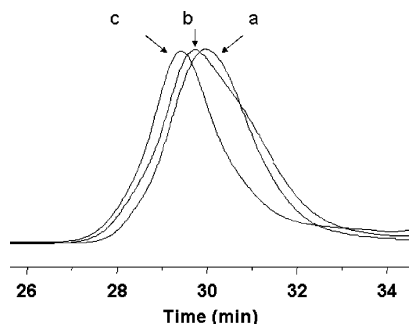
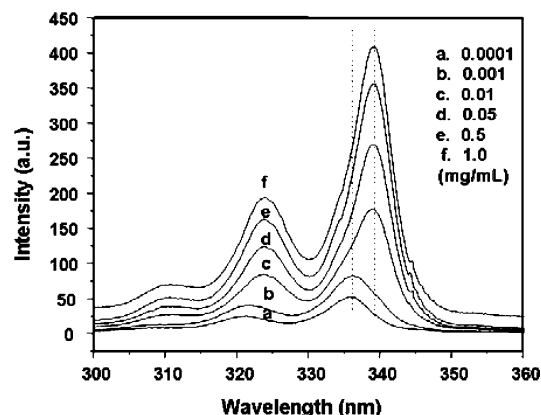
Moreover, to determine the sequence distribution of the two components in the copolymer, a ^{13}C NMR spectrum of the copolymer was measured. It has been reported previously that the resonances of carbons from carbonyl of ϵ -CL units are sensitive to chemical environment, namely sequence of backbone of copolymer. Multiple signals have been normally observed in the carbonyl region around 173 ppm of random copolymers of PCL.³² In this case, a single peak at 173.6 ppm in the carbonyl region shown in Figure 3 clearly indicated the diblock structure of this copolymer.

Molecular weights and molecular weight distributions were measured by GPC. Figure 4 shows GPC profiles of PCL precursor and block copolymers PCL-*b*-PPEG. Each chromatograph shows an unimodal peak and a relatively narrow polydispersity. The degree of polymerization of the PCL block is 62 which was calculated from the relative integration intensities of PCL methylene protons (f, Figure 1C) and protons from isopropyl group at one end of the polymer chain (a, Figure 1C). The actual molar ratio of the two components of the copolymer (PPEG/CL) was also estimated from the integrations of PCL methylene proton signal at 4.12 ppm (f, Figure 1C) and signal at 3.65 ppm assigned to methylene protons of mPEG brushes (g, Figure 1C). Detailed information of the copolymers was

Table 1. Results of Copolymerization of CL and PPEG

samples	feed ratio ^a [PPEG]/[CL]	DP ^b PPEG/CL	W _{PPEG} /W _{PCL} ^c (%)	M _n (g/mol) ^d (NMR)	M _n (g/mol) ^e (GPC)	M _w /M _n ^e (GPC)
PCL precursor	0:1	0/62	0/100	7 070	13 620	1.18
PCL- <i>b</i> -PPEG1	0.2:1	1.8/62	17.7/82.3	8 590	14 600	1.27
PCL- <i>b</i> -PPEG2	0.8:1	6/62	38.7/61.3	11 530	17 100	1.23

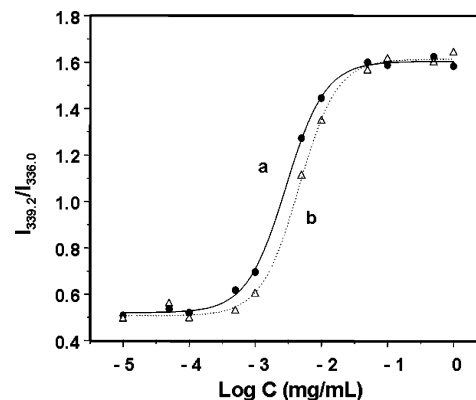
^a Molar feed ratio of the monomer PPEG to CL. ^b Degree of polymerization of PPEG and CL in the copolymer determined by ¹H NMR. ^c W_{PPEG} and W_{PCL} are the mass fractions of the PPEG and PCL segments in PCL-*b*-PPEG copolymers determined by ¹H NMR. ^d Determined by ¹H NMR. ^e Determined by GPC.

**Figure 4.** GPC chromatograms of (a) PCL precursor, (b) PCL-*b*-PPEG1, and (c) PCL-*b*-PPEG2.**Figure 5.** Excitation spectra at $\lambda_{em} = 390$ nm of pyrene at various concentrations of PCL-*b*-PPEG2.

summarized in Table 1. It is worth noting that the molecular weights of polymers by NMR are smaller than that determined by GPC, which is due to the fact that monodispersed polystyrene standards were used to generate the calibration curve in GPC analysis. Such phenomenon was also observed by many other groups in GPC analysis of PCL and its block copolymers.^{33–36}

It was found that the molecular weights and compositions of the copolymer were different at different feed ratios of the monomers. In fact, we also found that the number average molecular weight of PCL-*b*-PPEG increased linearly with the polymerization time up to 120 h. However, the conversion of the PPEG monomer was only around 10%, which was probably due to the higher equilibrium concentration of PPEG and its steric hindrance. The molecular weights calculated from NMR intergrations indicated that PCL-*b*-PPEG1 and PCL-*b*-PPEG2 contain 1.8 and 6 PEG brushes per polymer chain in average, respectively.

These diblock copolymers are amphiphilic and self-assemble into micelles in aqueous media. Pyrene was used as a fluorescence probe in this study to characterize the micellar formation of amphiphilic copolymers by determining its excitation spectra.^{37,38} As shown in Figure 5, a red shift of the (0,0) absorption band from 336.0 to 339.2 nm was observed in the excitation spectrum when the concentration of copolymer was increased.

**Figure 6.** Plot of the $I_{339.2}/I_{336.0}$ ratio (from pyrene excitation spectra) versus log C for (a) PCL-*b*-PPEG1, and (b) PCL-*b*-PPEG2 copolymer.**Table 2.** Properties of the PCL-*b*-PPEG Micelles

samples	CMC ^a (10^{-4} mg/mL)	mean diameter ^b (nm)	N _{agg} ^c
PCL- <i>b</i> -PPEG1	6.76	74 ± 5	247
PCL- <i>b</i> -PPEG2	13.80	85 ± 2	480

^a The critical micelle concentration (CMC) is determined by fluorescence technique using pyrene as a fluorescence probe. ^b Mean diameter determined by DLS. ^c N_{agg} was calculated according to $N_{agg} = M_{w,mic}/M_{w,unimers}$.

This red-shift results from the transfer of pyrene molecules from a water environment to the hydrophobic micellar core, and thus provides information on the location of the pyrene probe in the system, in fact, indicating the formation of micelles.³⁸

The CMC is a measurement describing the physical properties of the micelles and refers to the micelle thermodynamic stability.³⁹ As reported by Wilhelm et al., the concentration dependence of the $I_{339.2}/I_{336.0}$ ratios of the (0,0) band of pyrene was more sensitive to CMC than lifetime measurements or fluorescence emission.³⁷ In this case, it was also found that the intensities of the peaks were enhanced remarkably with increased polymer concentrations. The intensity ratios of $I_{339.2}/I_{336.0}$ from the excitation spectra were plotted against copolymer concentrations as shown in Figure 6. At low concentrations of copolymer, the total fluorescence intensity ratio remained nearly unchanged, taking the characteristic of pyrene in a water environment. As the concentration of the copolymer increased, the intensity ratio started to increase dramatically, reaching the characteristic of pyrene entirely in a hydrophobic environment at certain copolymer concentrations. This is a reflection of the whole process of micellization. From the sigmoidal shape curve, CMCs of the block copolymers were obtained and summarized in Table 2. It was found that CMC value increased from 6.76×10^{-4} to 13.80×10^{-4} mg/mL with the increase of PPEG content. The curves in Figure 6 also illustrated this phenomenon, namely, CMC of PCL-*b*-PPEG1 with less PPEG content was lower than that of PCL-*b*-PPEG2 which contains 38.7% of PPEG by weight. It is reasonable that the higher content of the

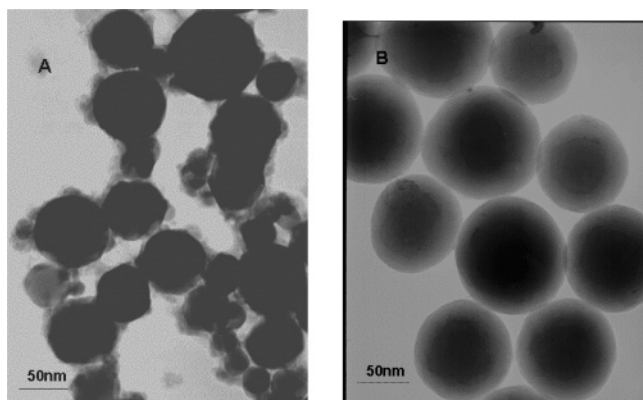


Figure 7. TEM images of (A) PCL-*b*-PPEG1 and (B) PCL-*b*-PPEG2 micelles.

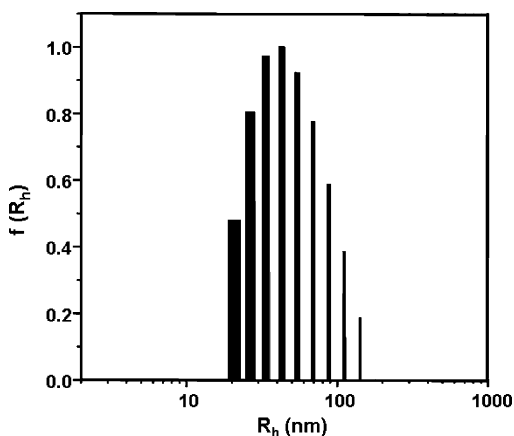


Figure 8. Particle size distribution of micelles formed by PCL-*b*-PPEG2 copolymer.

hydrophobic segments will result in stronger interactions between each other, leading to a more stable micellar structure and, therefore, to lower CMC value.

The successful formation of micelles was further confirmed by TEM measurement. Figure 7 shows the TEM image of the micelles formed by PCL-*b*-PPEG copolymers. It can be seen that the micelles take a spherical morphology. By close observation, the core-shell structure was evident, with the dark core composed of a high density of PCL and gray shell composed of a much lower density of PPEG. It is also observed from the TEM image that shell of PCL-*b*-PPEG2 with 6 PEG brushes is apparently thicker than that of PCL-*b*-PPEG1 with 1.8 PEG chains. As a typical example, the particle size distribution of PCL-*b*-PPEG2 micelles determined by dynamic light scattering was shown in Figure 8. Mean sizes of micelles formed by PCL-*b*-PPEG1 and PCL-*b*-PPEG2 copolymers are ca. 74 and 85 nm in diameter, respectively, which were basically consistent with those observed by TEM. The aggregation number of the copolymer molecules in the micellar structure was calculated using equation $N_{\text{agg}} = M_{\text{w,mic}}/M_{\text{w,unimers}}$ and listed in Table 2, where $M_{\text{w,mic}}$ and $M_{\text{w,unimers}}$ are the micelle molar mass determined by SLS and the molar mass of the individual diblock copolymer chain.⁴⁰

The in vitro degradation behavior of the PCL-*b*-PPEG2 micelles was evaluated at 37 °C at neutral pH and molecular weights of degradation products were analyzed by GPC. It is not surprising that polymer micelles alone could not degraded fast at neutral pH since both PCL and PPE have been demonstrated to degrade slowly at such conditions.^{41,42} In fact, in our experiments, only a very minor molecular weight decrease was observed after 45 days culture at pH 7.4 for PCL-*b*-PPEG2.

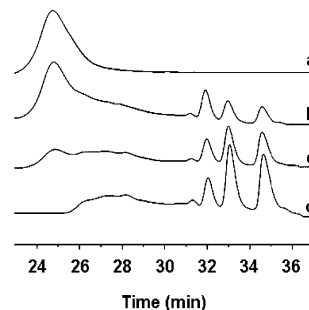


Figure 9. GPC chromatograms of PCL-*b*-PPEG2 at different degradation times (a) 0, (b) 2, (c) 16, and (d) 24 h in the presence of *Pseudomonas* lipase at 37 °C in phosphate buffer (0.05 M, pH 7.0).

However, in the presence of *Pseudomonas* lipase, a well-known enzyme to accelerate degradation of PCL,^{43,44} the molecular weights decreased rapidly. Figure 9 gives the GPC chromatograms of the degradation products in the presence of *Pseudomonas* lipase at different times at 37 °C. It is very clear that low molecular weight molecules were generated during 2 h of degradation with *Pseudomonas* lipase. The well resolved peaks eluted at 34.61, 33.03, and 32.03 min are likely from 6-hydroxycaproic acid, dimer and trimer, respectively.⁴⁵ With the increase of degradation time from 2 to 24 h, the intensity of peak from PCL-*b*-PPEG2 decreased significantly, whereas intensities of peaks from small molecules increased gradually, demonstrating the enzymatic degradation of the PCL block. However, there was no proof of PPE block degradation under *Pseudomonas* lipase enzyme catalysis until 24 h because of the absence of the PEG750 eluent peak that should be at 30.07 min. It is also worth noting that the retention time of the peak from PCL-*b*-PPEG2 in Figure 9, panels b and c, did not change during degradation, which may indicate that micelles were “eaten” by lipase in a one-by-one fashion, as observed by Gan et al. using laser light scattering measurements.⁴⁶

In summary, we have synthesized novel block copolymers based on biodegradable PCL and polyphosphoester. The structure of block copolymers has been well characterized. These block copolymers are amphiphilic and form a micellar structure in water, which was demonstrated by the fluorescence spectroscopic method using pyrene as a probe and further proven by TEM and DLS measurements. The copolymer micelles were biodegradable, which was demonstrated in the presence of *Pseudomonas* lipase. Through hydrophobic association between drug molecules with the hydrophobic core, the hydrophobic drug molecules could be loaded, and the micellar system based on the biodegradable brush-coil block copolymer is a potential drug carrier for pharmaceutical applications.

Acknowledgment. We are thankful for the financial support from the National Science Foundation of China (Contract 20504025) and the Bairen Program of the Chinese Academy of Sciences.

References and Notes

- (1) Allen, C.; Han, J. N.; Yu, Y. S.; Maysinger, D.; Eisenberg, A. *J. Controlled Release* **2000**, 63 (3), 275–286.
- (2) Scholz, C.; Iijima, M.; Nagasaki, Y.; Kataoka, K. *Polym. Adv. Technol.* **1998**, 9 (10–11), 768–776.
- (3) Otsuka, H.; Nagasaki, Y.; Kataoka, K. *Adv. Drug Delivery Rev.* **2003**, 55 (3), 403–419.
- (4) Hans, M.; Shimon, K.; Danino, D.; Siegel, S. J.; Lowman, A. *Biomacromolecules* **2005**, 6 (5), 2708–2717.
- (5) Najafi, F.; Sarbolouki, M. N. *Biomaterials* **2003**, 24 (7), 1175–1182.
- (6) Chang, Y.; Bender, J. D.; Phelps, M. V. B.; Allcock, H. R. *Biomacromolecules* **2002**, 3 (6), 1364–1369.

- (7) Shuai, X. T.; Merdan, T.; Unger, F.; Wittmar, M.; Kissel, T. *Macromolecules* **2003**, *36* (15), 5751–5759.
- (8) Allen, C.; Eisenberg, A.; Mrcic, J.; Maysinger, D. *Drug Delivery* **2000**, *7* (3), 139–145.
- (9) Nagasaki, Y.; Okada, T.; Scholz, C.; Iijima, M.; Kato, M.; Kataoka, K. *Macromolecules* **1998**, *31* (5), 1473–1479.
- (10) Arimura, H.; Ohya, Y.; Ouchi, T. *Biomacromolecules* **2005**, *6* (2), 720–725.
- (11) Allcock, H. R.; Powell, E. S.; Chang, Y. Y.; Kim, C. *Macromolecules* **2004**, *37* (19), 7163–7167.
- (12) Nakayama, M.; Okano, T. *Biomacromolecules* **2005**, *6* (4), 2320–2327.
- (13) Rijcken, C. J. F.; Veldhuis, T. F. J.; Ramzi, A.; Meeldijk, J. D.; van Nostrum, C. F.; Hennink, W. E. *Biomacromolecules* **2005**, *6* (4), 2343–2351.
- (14) Kakizawa, Y.; Furukawa, S.; Kataoka, K. *J. Controlled Release* **2004**, *97* (2), 345–356.
- (15) Arimura, H.; Ohya, Y.; Ouchi, T. *Biomacromolecules* **2005**, *6* (2), 720–725.
- (16) Yamamoto, Y.; Nagasaki, Y.; Kato, Y.; Sugiyama, Y.; Kataoka, K. *J. Controlled Release* **2001**, *77* (1–2), 27–38.
- (17) Yasugi, K.; Nakamura, T.; Nagasaki, Y.; Kato, M.; Kataoka, K. *Macromolecules* **1999**, *32* (24), 8024–8032.
- (18) Neiser, M. W.; Muth, S.; Kolb, U.; Harris, J. R.; Okuda, J.; Schmidt, M. *Angew. Chem.-Int. Ed.* **2004**, *43* (24), 3192–3195.
- (19) Khelfallah, N.; Gunari, N.; Karl, F.; Gkogkas, G.; Hadjichristidis, N.; Schmidt, M. *Macromol. Rapid Commun.* **2005**, *26*, 1693–1697.
- (20) Cheng, Z. P.; Zhu, X. L.; Kang, E. T.; Neoh, K. G. *Langmuir* **2005**, *21* (16), 7180–7185.
- (21) Sinha, V. R.; Bansal, K.; Kaushik, R.; Kumria, R.; Trehan, A. *Int. J. Pharm.* **2004**, *278* (1), 1–23.
- (22) Sun, H. F.; Mei, L.; Song, C. X.; Cui, X. M.; Wang, P. Y. *Biomaterials* **2006**, *27* (9), 1735–1740.
- (23) Forrest, M. L.; Won, C. Y.; Malick, A. W.; Kwon, G. S. *J. Controlled Release* **2006**, *110* (2), 370–377.
- (24) Zhao, Z.; Wang, J.; Mao, H. Q.; Leong, K. W. *Adv. Drug Delivery Rev.* **2003**, *55* (4), 483–499.
- (25) Wang, J.; Zhang, P. C.; Mao, H. Q.; Leong, K. W. *Gene Ther.* **2002**, *9* (18), 1254–1261.
- (26) Wang, S.; Wan, A. C. A.; Xu, X. Y.; Gao, S. J.; Mao, H. Q.; Leong, K. W.; Yu, H. *Biomaterials* **2001**, *22* (10), 1157–1169.
- (27) Wen, J.; Kim, G. J. A.; Leong, K. W. *J. Controlled Release* **2003**, *92* (1–2), 39–48.
- (28) Chen, D. P.; Wang, J. *Macromolecules* **2006**, *39* (2), 473–475.
- (29) Edmundson, R. S. *Chem. Ind.* **1962**, 1962, 1828–1829.
- (30) Duda, A.; Penczek, S. *Macromol. Rapid Commun.* **1995**, *16*, 67–76.
- (31) Tian, D.; Dubois, P.; Jerome, R. *Macromolecules* **1997**, *30* (7), 1947–1954.
- (32) Vanhoorne, P.; Dubois, P.; Jerome, R.; Teyssie, P. *Macromolecules* **1992**, *25* (1), 37–44.
- (33) Kricheldorf, H. R.; Eggerstedt, S. *Macromol. Chem. Phys.* **1998**, *199* (2), 283–290.
- (34) Duda, A.; Florjanczyk, Z.; Hofman, A.; Slomkowski, S.; Penczek, S. *Macromolecules* **1990**, *23* (6), 1640–1646.
- (35) Kricheldorf, H. R.; Bornhorst, K.; Hachmann-Thiessen, H. *Macromolecules* **2005**, *38* (12), 5017–5024.
- (36) Save, M.; Schappacher, M.; Soum, A. *Macromol. Chem. Phys.* **2002**, *203* (5–6), 889–899.
- (37) Wilhelm, M.; Zhao, C. L.; Wang, Y. C.; Xu, R. L.; Winnik, M. A.; Mura, J. L.; Riess, G.; Croucher, M. D. *Macromolecules* **1991**, *24* (5), 1033–1040.
- (38) Zhao, C. L.; Winnik, M. A.; Riess, G.; Croucher, M. D. *Langmuir* **1990**, *6* (2), 514–516.
- (39) Kwon, G.; Naito, M.; Yokoyama, M.; Okano, T.; Sakurai, Y.; Kataoka, K. *Langmuir* **1993**, *9* (4), 945–949.
- (40) Giacomelli, C.; Le Men, L.; Borsali, R.; Lai-Kee-Him, J.; Brisson, A.; Armes, S. P.; Lewis, A. L. *Biomacromolecules* **2006**, *7* (3), 817–828.
- (41) Baran, J.; Penczek, S. *Macromolecules* **1995**, *28* (15), 5167–5176.
- (42) Gan, Z. H.; Liang, Q. Z.; Zhang, J.; Jing, X. B. *Polym. Degrad. Stab.* **1997**, *56* (2), 209–213.
- (43) Li, S. M.; Garreau, H.; Pauvert, B.; McGrath, J.; Toniolo, A.; Vert, M. *Biomacromolecules* **2002**, *3* (3), 525–530.
- (44) Li, S. M.; Pignol, M.; Gasc, F.; Vert, M. *Macromolecules* **2004**, *37* (26), 9798–9803.
- (45) Geng, Y.; Discher, D. E. *J. Am. Chem. Soc.* **2005**, *127* (37), 12780–12781.
- (46) Gan, Z. H.; Jim, T. F.; Li, M.; Yuer, Z.; Wang, S. G.; Wu, C. *Macromolecules* **1999**, *32* (3), 590–594.

BM051003C